ELSEVIER

Tectonophysics 308 (1999) 487–502

TECTONOPHYSICS

www.elsevier.com/locate/tecto

Present and recent stress regime in the eastern part of the Pyrenees

X. Goula [a,*], C. Olivera [a], J. Fleta [a], B. Grellet [b], R. Lindo [c], L.A. Rivera [d], A. Cisternas [d], D. Carbon [b]

[a] *Servei Geològic de Catalunya, Institut Cartogràfic de Catalunya, Parc de Montjuic, s.n., E-08038 Barcelona, Spain*
[b] *GEOTER, 3 rue Jean Monnet, 34810 Clapiers, France*
[c] *Departamento de Geofísica, Facultad de Físicas, Universidad Complutense, Cindad Universitaria, 28040 Madrid, Spain*
[d] *Institut de Physique du Globe, 5 rue René Descartes, 67084 Strasbourg Cedex, France*

Received 10 June 1998; accepted 26 March 1999

Abstract

Earthquake focal mechanisms and microtectonic analysis of fault striation are presented in order to study the regional state of stress in the eastern part of the Pyrenees. The inversion of these data, carried out independently, shows a submeridian direction of the maximum horizontal stress, remaining stable since the Plio–Quaternary until present time. This analysis confirms the evolution of the regional stress from an extension regime at the end of the Aquitanian period to a regime presently characterised either by an intermediate (strike-slip) or by a compression stress regime.

Keywords: Pyrenees; seismicity; neotectonics; stress tensor

1. Introduction

The passive margins of the Gulf of Lion and Valencia trough, correspond to the western margin of the Algero-Provençal basin which opened due to the Oligo-Aquitanian rifting, but also to the Burdigalian oceanic accretion associated with the southeastward drifting of the Corsica–Sardinia block. This extensional episode is linked to back-arc opening in the context of African and European plate convergence (Fig. 1A) (Bois, 1993; Pascal et al., 1993; Mauffret et al., 1995; Olivet, 1996). Extensional faulting affects the pre-rift Mesozoic cover, which is detached above the Palaeozoic basement, the latter one being undeformed during the rifting. Inland, the margin is bounded by several inherited NE–SW major faults (Cevennes, Nîmes, Têt and Vallès–Penedès faults), which limit a system of half-graben basins (Guimerà, 1984; Villeger, 1984; Roca and Guimerà, 1992; Bois, 1993; Pascal et al., 1993; Roca, 1994).

The structure of the Gulf of Lion, mainly offshore, is segmented by several NW–SE transfer faults and can be divided into a northeast domain, where the grabens trending N030 are narrow, and a southwest domain characterised by two 7 to 8 km deep depressions (Mauffret et al., 1995). The transition zone between the Gulf of Lion structures and the Catalan margin structures corresponds to a major NW–SE transfer zone (Catalan transfer zone). A NNE–SSW to N–S trend is observed in the northern part of the steep and narrow Catalan coastal margin, in contrast with the E–W and NE–SW orientations which characterise the Catalan grabens of the southern margin.

* Corresponding author. Tel.: +34-93-425-2900/x3264; Fax: +34-93-426-7442; E-mail: xgoula@icc.es

0040-1951/99/$ – see front matter
PII: S0040-1951(99)00120-1

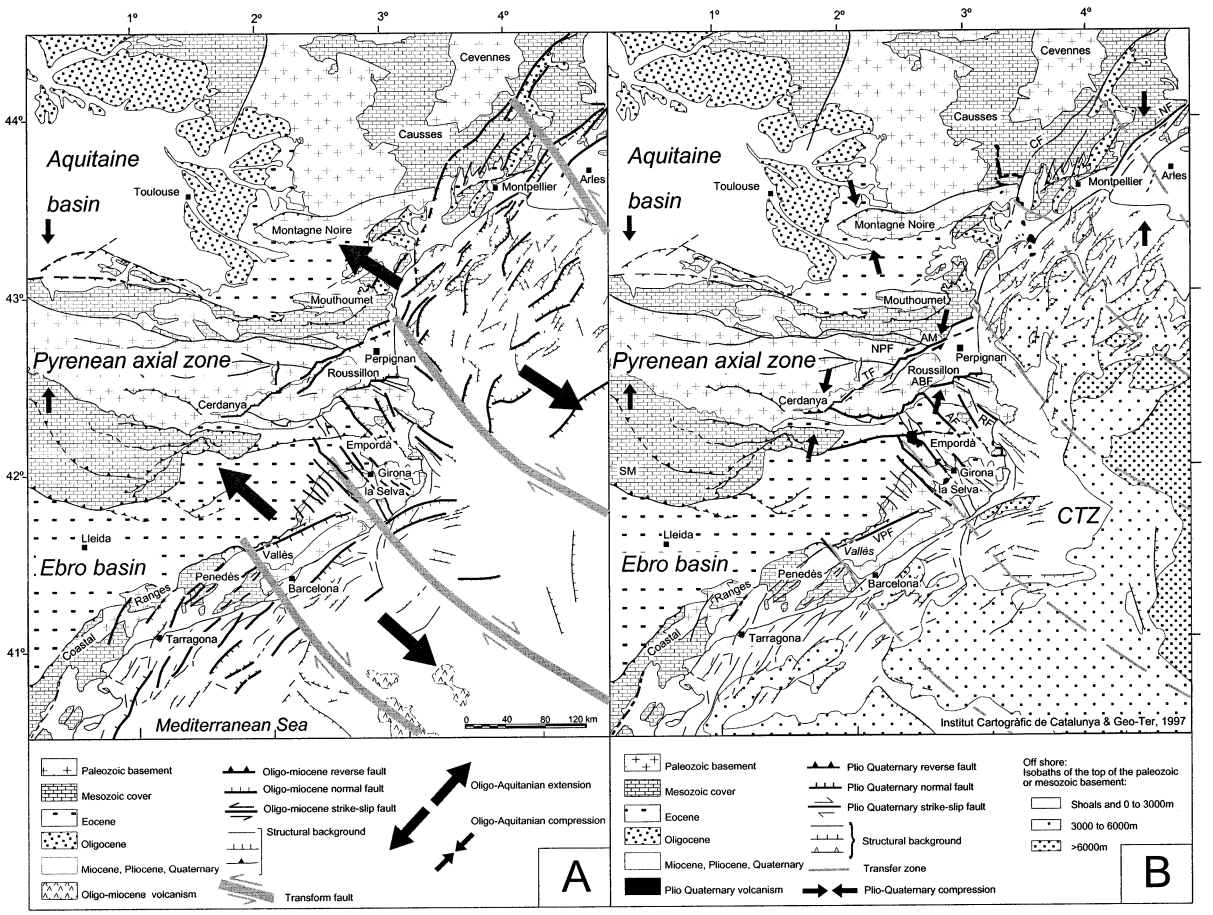

Fig. 1. Structural background of the eastern Pyrenees and northwestern part of the Mediterranean Sea: (A) during the Oligo-Miocene period; (B) Plio-Quaternary. *ABF* = Alberes fault; *AF* = Albanyà fault; *AM* = Agly massif; *CF* = Cevennes fault; *CTZ* = Catalan transfer zone; *NF* = Nîmes fault; *NPF* = North Pyrenean fault; *RF* = Roses fault; *SM* = Sierras Marginales; *TF* = Têt fault; *VPF* = Vallès–Penedès fault.

Inland, in the eastern part of the Pyrenees, the Oligo-Aquitanian extension episode corresponds to the opening of three deep sedimentary basins along major normal faults: (a) the Roussillon graben bounded to the north by the NE–SW Têt fault and to the south by the ENE–WSW Alberes fault which limits the Palaeozoic Alberes massif; (b) the Empordà basin, trending NW–SE, limited by the Albanyà and the Roses faults; (c) the Vallès–Penedès graben, trending ENE–WSW.

The western limit of the region of influence of the rifting is assumed to correspond to the Miocene Cerdanya half-graben, which is filled with more than 900 m of Neogene sediments.

The stress regime associated with the rifting, and deduced from microtectonics measurements, indicates a horizontal minimum stress σ_3 trending NW–SE in Languedoc-Roussillon (Arthaud et al., 1981) and a slightly different orientation (WNW–ESE) in Empordà and Vallès–Penedès (Roca and Guimerà, 1992; Roca, 1994). The central and western part of the Pyrenees are still in a compressive stress regime during the same period (Simón, 1984; Cortés et al., 1996).

The southeastward drifting of the Corsica–Sardinia block stopped at the end of Burdigalian time. Since that time, the tectonic regime in the western part of the Mediterranean Sea gradually changed from extension to compression due to the effects of the N–S convergence between the African and Euro-

pean plates. This modification of the stress regime is not synchronous at the scale of the Gulf of Lion and the Catalan margin. The first evidence of deformation under compression appear: (a) in the northern part (Ventoux–Lure area) during the Late Miocene (Serravallian) (Villeger, 1984); (b) in Languedoc-Roussillon during the Early Pliocene; and (c) in Catalonia at the end of the Pliocene (Fig. 1B). The NE–SW (Nîmes, Têt faults) Oligo-Aquitanian normal faults seem to have been reactivated with a predominant reverse sinistral strike-slip component, while the E–W segments show mostly pure reverse faulting, even though the intensity of deformation remains moderate (Philip et al., 1991; Grellet et al., 1993; Fleta et al., 1996).

Although tectonic and seismic deformation are moderate in the eastern part of the Pyrenees, it was possible to collect accurate data concerning earthquakes recorded during the recent years, which are representative of present-day tectonic stresses. Moreover, detailed field analysis enabled us to find fault plane striations in Plio-Quaternary sediments. The main objective of this study is to determine the recent to present state of stress, and to compare it to the Oligo-Miocene extension regime. Two complementary sets of data have been chosen, representing the most accurate and direct records of the tectonic deformation. First, focal mechanisms which provide information on the present-day stress field, and second, selected microtectonic data which give the most recent (Plio-Quaternary) state of stress. The two collections of data were processed separately, by using recent numerical inversion methods, in order to perform a joint analysis of the regional stress tensors obtained.

2. Microtectonic analysis

The influence of Neogene volcanism is taken into account as an evidence of the opening of the central European rift during the Oligo-Aquitanian period, independently of the geological location of neotectonic activity. In the same way, the presence or absence of a Triassic to Tertiary evaporitic substratum, possibly related to halokinetic local phenomena, is analysed. The amount of deformation of the folded cover in the Ebro foreland is also studied.

2.1. Microtectonic data

Microtectonic analysis of post-Miocene sediments has been performed by using data from 23 microtectonic sites. The data correspond to measurements of striation and sense of motion along a population of fault planes. Most of the measurements are situated in places around the margins of the Neogene basins (in the eastern part of the Pyrenees, in particular, where an interaction exists between the E–W oriented Pyrenean structures, and those associated to Neogene and Quaternary volcanism which are oriented NW–SE). Nevertheless, some of the data correspond to the Ebro basin along the thrust front of the southern Pyrenees. Thus, the study sites concentrate along the Neogene basins of Cerdanya, Roussillon, Empordà, Têt and North Pyrenean faults, with some isolated additional sites distributed along the Mediterranean system (Fig. 2).

Table 1 shows the main geologic and structural characteristics of the 23 sites investigated, including the measurements of striations at each site, and the stress regime obtained by inversion of the data, whenever it was possible (Fig. 2). The quality, quantity and the geological location of the data are variable. In principle, sites with more than five striae (15 sites) are used in order to make a quantitative determination of the stress tensor regime (Etchecopar, 1984).

A synthetic description of each of the microtectonic sites has been performed. Three of these descriptions are presented in Fig. 3: (a) the reactivation of the southern margin of the Cerdanya basin in reverse faulting (site of Nas); (b) one of the most important Plio-Quaternary strike-slip faults of the Pyrenean area, along the western margin of the Empordà Neogene basin (site of Incarcal); (c) a reverse fault with an accumulated displacement of over 10 m, in the Ebro depression (site of Canelles), on the northern flank of the Canelles diapir, over the Mesozoic units of the Sierras Marginales.

2.2. Determination of the regional stress tensors

The basic inverse method used for the determination of stress tensors from the analysis of fault striations is that of Etchecopar (Etchecopar et al., 1981; Etchecopar, 1984). In this method, a great number of tensors is generated by using randomly

Table 1
Microtectonic study sites description

No	NAME / NEOGENE CONTEXT	GEOLOGICAL LEVEL AFFECTED	TYPE OF DEFORMATION	E	V	MICROTECTONIC DATA -STRIAE-	STRESS TENSOR	COMMENTS
1	NAS CERDANYA	Contact between paleozoic substratum and mio-pliocene conglomerates. Microtectonics measurements in the Pliocene levels	Major miocene E-W normal fault on the southern rim of the Cerdanya half graben reactivated as a reverse fault during the plio-quaternary compressive episode.	N	N	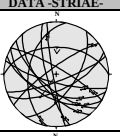	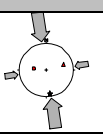	Compressional regime σ_1= 171.4 / 12.0 σ_2= 277.3 / 52.2 σ_3= 72.7 / 35.2 r= 0.45 n=12
2	MARTINET CERDANYA	Contact between the würmian terrace of the Segre river and Paleozoic units	Thrusting of paleozoic (silurian) gneisses over the quaternary conglomeratess. The major plane is trending WNW-ESE, underlined by clay and gouge. The pebbles, along the fault plane are truncated and striated	N	N	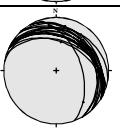	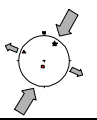	Strike slip regime σ_1= 39.1 / 17.5 σ_2= 189.7 / 70.1 σ_3= 306.2 / 9.2 r= 0.08 n=15
3	ESTAVAR CERDANYA	Contact between continental miocene clay and sand and würmian alluvial deposits (sand, gravels and conglomerates)	Reverse NW-SE faults between miocene levels and the würmian Rio Segre terrace	N	N	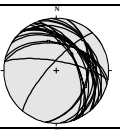	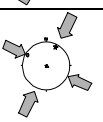	Compressional regime σ_1= 30.0 / 4.7 σ_2= 120.2 / 1.9 σ_3= 233.3 / 85.2 r= 0.54 Offset > 2m n=19
4	PALAU CERDANYA	Contact between paleozoic shales and late Pleistocene alluvial terrace	Normal faults trending NNE and NNW	N	N	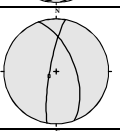		Only two planes were measured Offset <5m n=2
5	ILLE SUR TET ROUSSILLON	Pliocene continental facies: loams, gravels and clays	Sinistral reverse faulting on a segment of the Têt fault trending NE	N	N	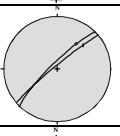		Only two sinistral reverse faults were measured. They correspond to the superficial expression of the major NE-SW Têt fault. Vertical offset close to 1m n=2
6	NEFIACH ROUSSILLON	Pliocene deltaic facies. Sand, gravels and pebbles typical of the marine-continental transition zone	Sinistral strike-slip fault trending NNE, parallel to the Têt fault	N	N	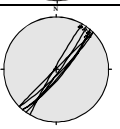	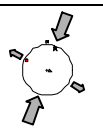	Strike-slip regime σ_1= 015.0 / 5.0 σ_2= 165.8 / 84.3 σ_3= 284.8 / 2.8 r= 0.64 n=6
7	CARAMANY AGLY MASSIF	Quaternary colluvium, silts and conglomerate	Quaternary reverse fault in the Agly massif between colluvium and paleozoic gneiss	N	N	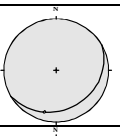		Only one plane was measured Offset >10 m n=1
8	TROUILLAS ROUSSILLON	Lacustrine upper Pliocene: limestones, clay and sands	Normal NNE faults which affect the upper Pliocene levels inside the Roussillon basin	N	N	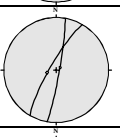		Two major submeridian normal faults in the middle of the Roussillon neogene basin Offset >70m n=2
9	MONTESQUIEU ROUSSILLON	Continental miocene clay and pebbles	Reverse E-W fault between paleozoic shales and miocene levels	N	N	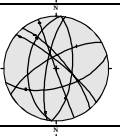	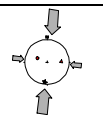	Uniaxial compression σ_1= 184.7 / 0.1 σ_2= 94.7 / 0.5 σ_3= 285.9 / 89.5 r= 0.01 n=8
10	MAUREILLAS ROUSSILLON	Continental upper Miocene conglomerate	Strike-slip faults trending NNE	N	N	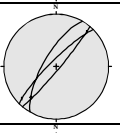		Three strike-slip planes were measured along a major NE-SW structure which offsets (sinistral component) for more than 1 km the southern border of the Roussillon basin n=3
11	MONTGO EMPORDA	Post-miocene conglomerates located on mesozoic calcareous cover	Post-Miocene E-W strike slip fault on the northern margin of Montgri allochonous mesozoic cover unit	N	Y M	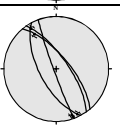	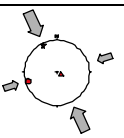	Uniaxial compression σ_1= 334.0 / 6.7 σ_2= 252.8 / 9.5 σ_3= 108.6 / 78.4 r= 0.07 n=5
12	INCARCAL EMPORDA	Plio-Quaternary lacustrine serie. Calcareous sands and muds with high vertebral fauna contents	Major dextral strike-slip faults trending NNW. They are associated with minor submeridian normal faults, E-W flexures and sediment filling karstic dolines in the major Albanya fault context. Tensor solution was obtained with strike-slip faults only	Y E	N	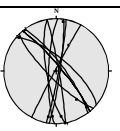	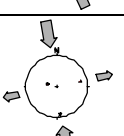	Uniaxial compression σ_1= 172.7 / 9.7 σ_2= 283.9 / 64.7 σ_3= 78.5 / 23.1 r= 0.00 Minor hydroplastic normal faults seems to be due to local collapse effects n=11

Table 1 (continued)

No	NAME / NEOGENE CONTEXT	GEOLOGICAL LEVEL AFFECTED	TYPE OF DEFORMATION	E	V	MICROTECTONIC DATA -STRIAE-	STRESS TENSOR	COMMENTS
13	CRESPIA EMPORDA	Pliocene alluvial facies of conglomerates, sands and clays	Normal fault on a segment of the Albanyà fault system trending NW-SE	Y E	N	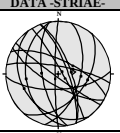	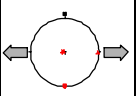	Extensional regime σ_1= 297.4 / 84.5 σ_2= 180.2 / 2.5 σ_3= 90.0 / 4.9 r= 0.54 Offset > 2m n=13
14	RAJOLINS EMPORDA	Plio-Quaternary alluvial facies of conglomerates, sands and clays with volcanic pebbles	Dextral reverse NW-NE faults	Y E	Y Q	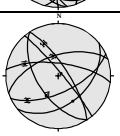	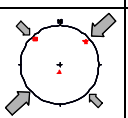	Compressional regime σ_1= 248.3 / 12.6 σ_2= 180.2 / 10.4 σ_3= 187.4 / 73.6 r= 0.56 n=7
15	TORTELLA EMPORDA	Late Quaternary alluvial facies of gravels and clays	Reverse NNE - SSW faults	Y E	Y Q	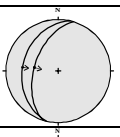		The two available microtectonics data are pure reverse faults. On the same site, the plio-Quaternary serie is folded. Offset > 1m n=2
16	CAMOS EMPORDA	Plio-Quaternary alluvial facies of gravels and clays	NW-SE Camós-Celrà normal fault and roll-over structures	Y E	N	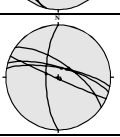	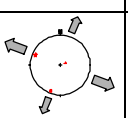	WNW-ESE extensional regime n=5
17	SERINYA EMPORDA	Quaternary terrace of the Sert river, gravels, sands and clay	Quaternary terrace affected by normal faults in the E-W Vallfogona thrust context. These normal faults are located in a quarry a hundred meters north of quaternary anticline affected by a major reverse fault (095 S 65)	Y E	N	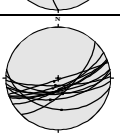	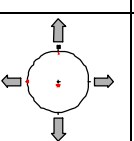	Extensional radial regime σ_1= 179.1 / 79.6 σ_2= 270.4 / 0.2 σ_3= 0.4 / 10.4 r= 0.02 n=14
18	CAIXANS EMPORDA	Pliocene alluvial facies of gravels and clays	Normal faults on a segment of the Albanyà fault trending NW-SE	Y E	N	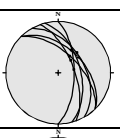	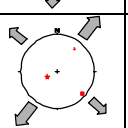	Extensional regime σ_1= 241.5 / 63.9 σ_2= 131.3 / 9.6 σ_3= 37.0 / 24.0 r= 0.52 Cumulated offset >100m n=6
19	CALLUS EBRO	Quaternary terrace of Cardener river	NE-SW reverse faults affecting a quaternary terrace on the Callús gypsum anticline	Y Q	N	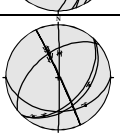	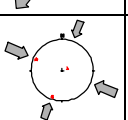	Compressional regime σ_1= 292.0 / 10.6 σ_2= 200.3 / 9.2 σ_3= 70.8 / 75.7 r= 0.69 Offset >1m n=9
20	AGER EBRO BASIN/ ALLOCTHONOUS COVER	Plio-Quaternary alluvial fan	Quaternary terrace affected by an E-W reverse fault in the northern flank of the Balaguer gypsum anticline	Y Q	N	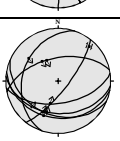	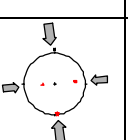	Compressional regime σ_1= 174.7 / 2.8 σ_2= 83.0 / 32.3 σ_3= 269.2 / 57.6 r= 0.52 Offset >1m n=9
21	CANELLES ALLOCTHONOUS COVER	Quaternary terrace of Noguera Ribagorçana river	NW-SE reverse fault affecting a quaternary terrace in the northern flank of the Canelles triassic diapir	Y T	N	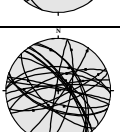	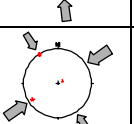	Compressional radial regime σ_1= 237.1 / 12.2 σ_2= 327.5 / 1.9 σ_3= 66.1 / 77.6 r= 0.89 Offset >10m n=19
22	CASTELLBISBAL BAIX LLOBREGAT	Plio-Quaternary clays and sands series	NW-SE reverse faults, meridian normal faults and flexures affecting plio-quaternary sediments	N	N	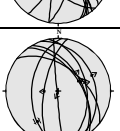		NE-SW qualitative compressional regime. No striae available. These observations were made along the major Llobregat NW-SE strike slip fault n=8
23	MONTREDO BAIX EBRE	Quaternary terrace of Ebro river	Meridian normal faults affecting a quaternary terrace	N	N	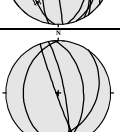		WSW-ESE extensional regime from Julià and Santanach (1980) and Masana (1995) No striae n=5

Name, location, geological level affected, type of deformation, evaporitic levels (Column E: Presence (Y) or absence (N) of evaporite levels of Eocene (E), Triassic (T) or Oligocene (O) period), volcanism activity (Column V: Presence (Y) or absence (N) of volcanism activity of Miocene (M) or Plio-Quaternary (Q) period), microtectonic data stereogram, individual calculated stress tensor, and comments (parameters of the calculated stress tensor, cumulated offset along the fault plane, etc.). No. 23: sources Julià and Santanach (1980) and Masana (1995).

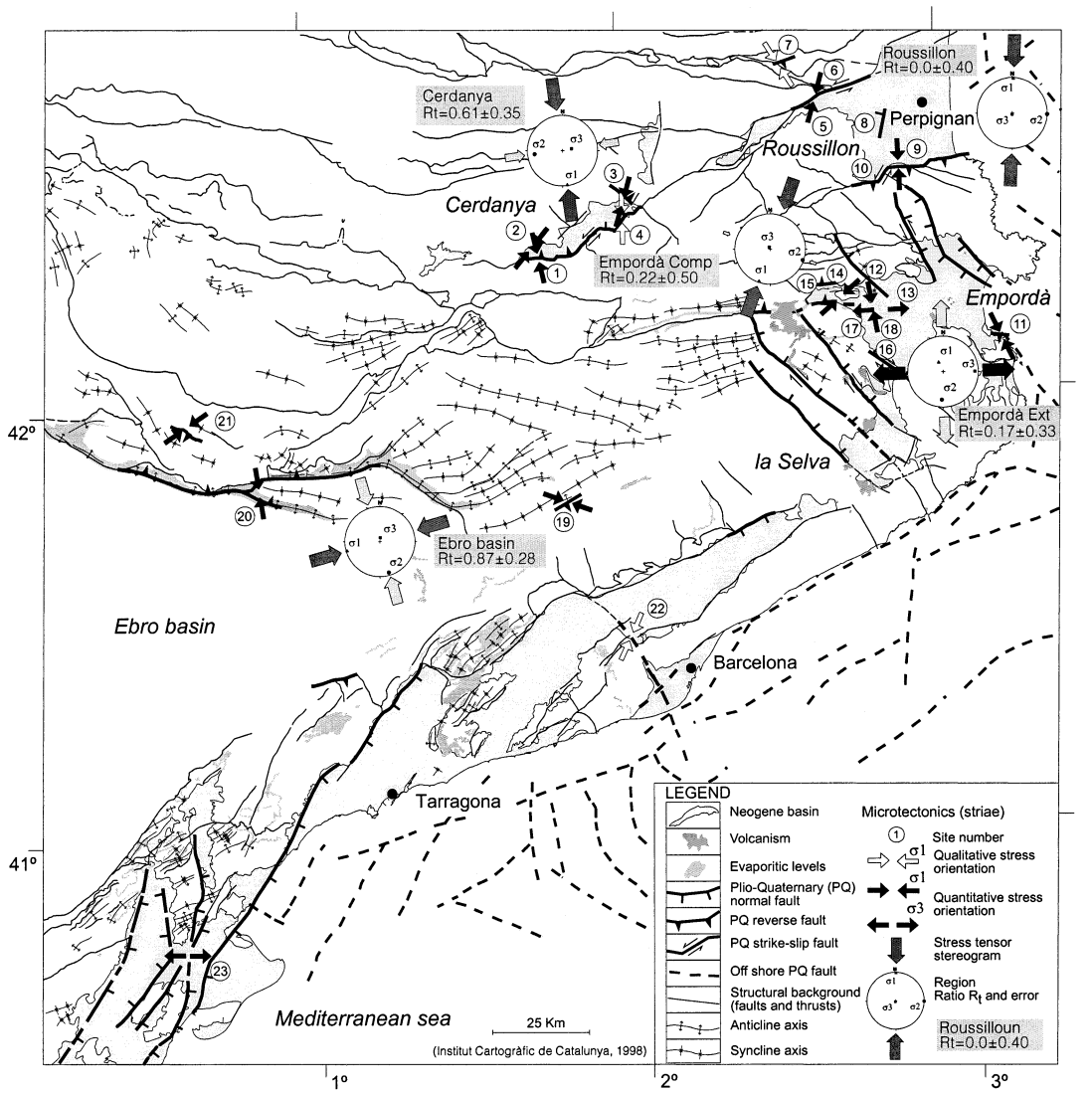

Fig. 2. Microtectonic sites location in the neotectonic framework of the eastern part of the Pyrenees with the deduced stress tensor (for each site and by zones). Qualitative stress orientation corresponds to sites with insufficient striation measurements.

chosen parameters (ψ, θ, ϕ, R_t), with a stress form factor defined by $R_t = (\sigma_2 - \sigma_3)/(\sigma_1 - \sigma_3)$. Then, for each one of these tensors, one calculates the associated theoretical striation direction for each one of N fault planes. Then, the method selects the n fault planes ($n < N$) which give the smallest angles between the theoretical and actual striations. In practice, the striations with differences greater than 45º are rejected. Finally, the sum S of the absolute value of these n angular deviations is calculated. The tensor with the smallest value of S among all these tensors, is chosen to be the optimal one.

Fig. 3. Synthetic description of three of the most representative brittle deformation sites, composed by a photo, a geological cross section, a geological description and main results of the microtectonics analysis. (a) 1 – Nas; (b) 12 - Incarcal; and (c) 21 – Canelles.

1 NAS (Cerdanya basin) (a)

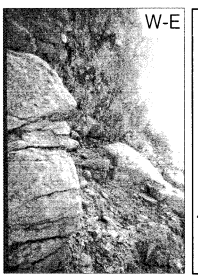

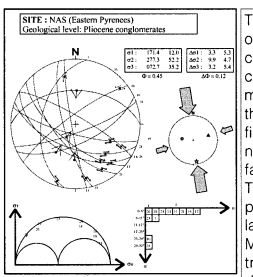

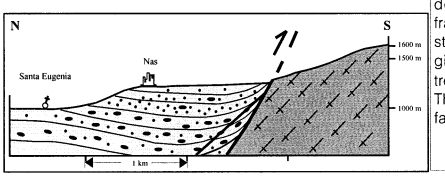

This outcrop is located in the southern rim of the Cerdanya half graben close to the city of Bellver (Spain). The mio-pliocene conglomerates are verticalised along the major E-W normal fault planes which limit the paleozoic shales and the neogene filling of the basin. The synsedimentary normal movements are attested by the fan shaped conglomerate deposits. These faults were reactivated with a predominant reverse component during late Pliocene and Quaternary.
Most of the pebbles are reversely truncated along a broad zone of deformation. Measurements of the fracturation patterns on the pebbles and striations analysis along the fault planes give a horizontal maximum stress σ_1 trending N170.
These observations of reactivated E-W fault planes are frequent in this area.

12 INCARCAL (Empordà basin) (b)

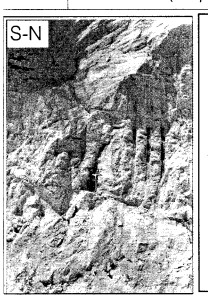

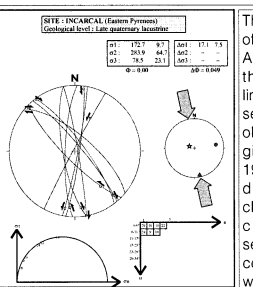

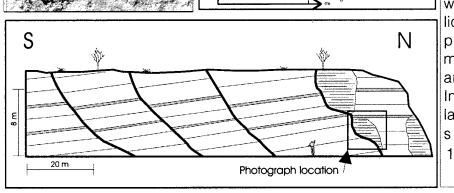

This site is located on the western margin of the Empordà neogene basin within the Albanyà normal fault context. The thickness of the Plio-Quaternary limestones sands and muds lacustrine series is larger than 70 m. Datation was obtained on vegetal and faunal rests and give an age of 2.1-1.6 MY BP (Roiron, 1983). Two tectonic episodes are differentiated. The first one is characterized by an extensive regime contemporaneous with the sedimentation and the second one, later, corresponds to a compressive regime with a general NE tilting, slumping, liquefaction, W-E flexures and faulting processes. NW-SE normal faults and major NNW-SSE dextral strike-slip faults are located on the cross section. Inversion was performed only with the late major strike-slip faults and give a strike-slip regime with σ_1 172/9 and σ_3 78/23.

21 CANELLES (Noguera Ribagorçana - Ebro basin) (c)

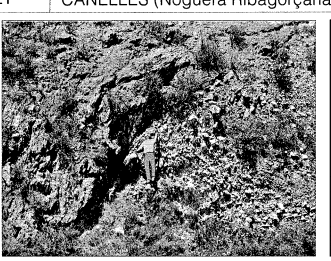

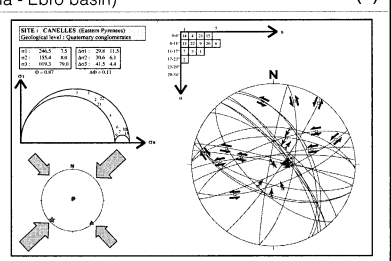

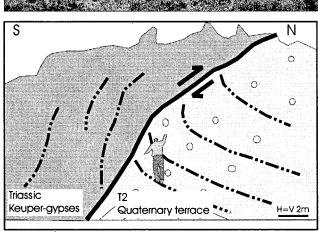

This site is located in the northern flank of the Canelles triassic diapir on the mesozoic cover allochonous units of the Sierras Marginales (SM) close to Castellonroi village. The gypsum of Keuper facies are thrusting a Quaternary terrace of Noguera Ribagorçana river (T2) by a N135 dextral reverse fault with more than 20 m of offset. The microtectonic analysis of striations on the pebbles along the fault plane gives a compressional regime with σ_1 sub horizontal trending NE-SW.

In a first step, we tried to explain the whole data set selected for the inversion of the stress tensors at each site (177 striae for 21 sites), by a unique regional stress tensor. This first inversion gave a tensor corresponding to a regime in compression, with a NNW–SSE oriented maximum horizontal stress, a result which was badly constrained.

In a second step, and in order to improve the inversion, we took into account the geological characteristics (local presence of evaporitic levels or volcanism, see Table 1) and, in particular, the indications given by the individual stress tensors, to try to determine a state of stress coherent for each zone (Fig. 2). For example, in the Cerdanya basin, more than 80% of the faults are explained by a compression tensor ($R_t = 0.61 \pm 0.32$) with σ_1 trending N–S. For the Neogene Roussillon basin, 86% of the faults are explained by a compression or strike-slip tensor ($R_t = 0.0 \pm 0.4$) with σ_1 still trending N–S. In the Ebro basin, 70% of the faults are consistent with a radial compression ($R_t = 0.87 \pm 0.28$) and finally, in Empordà, 68% of the data are consistent with a radial extension ($R_t = 0.17 \pm 0.33$), the remaining faults being explained by a compression, or strike-slip tensor ($R_t = 0.22 \pm 0.50$) with σ_1 close to NNE–SSW.

The results obtained above give a relatively homogeneous stress field, characterised by the predominant N–S orientation of σ_1, which corresponds to a compressional or strike-slip regime, except for local variations of the R_t ratio in the Ebro basin, and for an extensional regime in the Empordà basin.

The presence of superficial evaporitic levels can induce non-tectonic deformations in the Ebro basin, which may alter the results. On the other hand, the two different states of stress which resulted from the inversion in Empordà, may reflect two successive tectonic episodes: the extensional deformations affecting the Pliocene conglomerates (sites 12, 13, 16 and 18) seem to be older than the reverse and strike-slip faulting observed in Quaternary lacustrine deposits (sites 11, 12, 14 and 15). The radial extension evidenced in a Quaternary terrace (site 17) may be attributed to a local perturbation on the regional Quaternary stress field due to the presence of superficial evaporitic levels.

A good example of this relative chronology is illustrated in the Incarcal quarry (site No. 12), where the Upper Pliocene clay levels are affected by small listric normal faults, while the overlying Quaternary lacustrine limestones are essentially affected by major NNW–SSE dextral strike-slip faults (Fleta et al., 1996).

3. Regional seismicity

Although present-day seismicity of the eastern part of the Pyrenees is moderate, in agreement with the low deformation rate of the region, important earthquakes took place in the past. Namely, a destructive earthquake of intensity VIII–IX MSK (Olivera et al., 1994) occurred in the central Pyrenees in 1373. Later on, a series of earthquakes caused considerable damages over a large area of the eastern Pyrenees, extending from the southern part of the Palaeozoic axial zone to the northern part of the Catalan coastal ranges, during the period 1427–1428 (Banda and Correig, 1984; Olivera et al., 1999).

Instrumental seismicity is rather scarce. Seismological Observatories were set up early in the century in the studied area, but it is only since 1976, when the first station was installed by Laboratoire de Detection et de Géophysique (LDG, France) in the Pyrenees, that a better survey of the region was possible. In fact, it is only since 1985 that a network formed by a sizeable number of stations was installed and became operational in Catalonia and southern France. We may consider then two periods. The first one (1977–1985) is characterised by few stations and hence poor resolution for the epicentral determinations (errors of the order of 10 km) and badly constrained depths. For this period we consider the data obtained by the Servei Geològic de Catalunya (SGC), and completed by the observations of the LDG. For the second period (1986–1996), the network becomes denser in the region of the Pyrenees (Souriau and Pauchet, 1998). The mean distance between stations becomes about 30 km, and the earthquakes located within the network have an accuracy of 2–3 km for the epicentre, and 5 km for the depth. We used the SGC database for this second period including, in particular, the common hypocentral determinations performed by the SGC and the Observatoire Midi-Pyrénées (OMP) of Toulouse compiled in the Seismic Activity in the Pyrenees Annual Bulletins (SGC/OMP, 1990–1996).

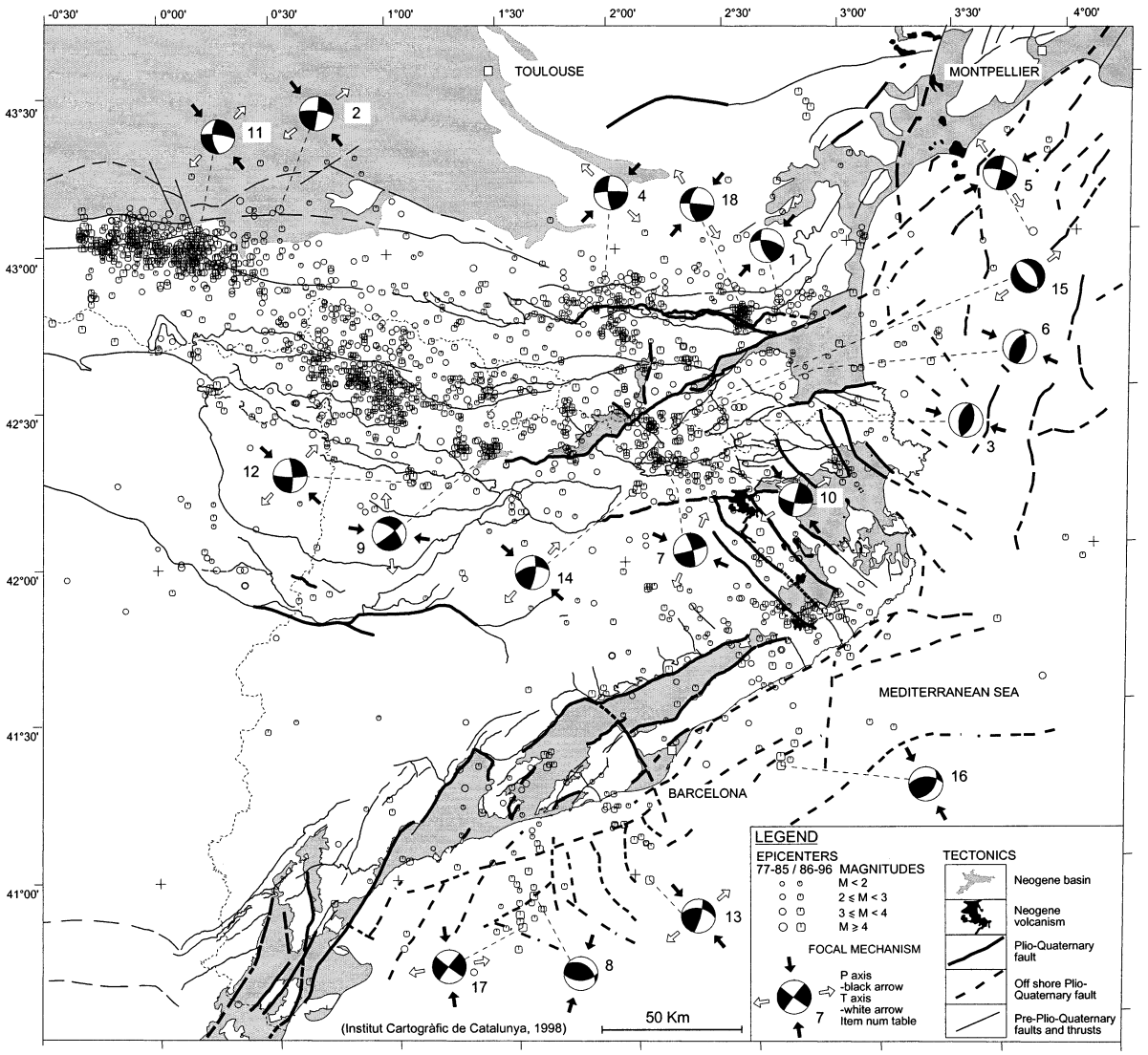

Fig. 4. Seismicity 1977–1996 with focal mechanisms obtained by different authors for 18 earthquakes on a schematic structural background (see Table 2).

The seismicity corresponding to the period 1977–1996 together with the focal mechanisms and the tectonic context of the area are presented in Fig. 4. The main features characterising the seismicity are: (a) the seismic activity is mainly located in the Pyrenees and in the Mediterranean area; in the Ebro basin the activity is very low in agreement with the scarce tectonic deformation observed; (b) in spite of the density of seismic stations after 1985, there is still an incomplete azimuthal coverage for earthquakes located in the Mediterranean system (Catalan coastal ranges and continental platform). These determinations are not as precise as those of Pyrenean earthquakes. Although the seismicity in the Mediterranean system is lower than in the Pyrenees, 7 out of the 11 earthquakes with magnitude larger than 4 have occurred there during the period 1986–1996, offshore mainly; (c) most of the earthquakes in the Pyrenees are concentrated in the axial zone. Although the seismic activity in the eastern Pyrenees

is lower than in the central Pyrenees, the strongest earthquake for the period of study occurred in 1996 in the eastern Pyrenees, with $M = 5.2$ and a great number of aftershocks (Olivera et al., 1996; Rigo et al., 1997).

4. Focal mechanisms and stress field

4.1. Data on mechanisms

We started the study with a collection of 30 earthquakes within the period 1969–1996. Their hypocentral parameters and other characteristics are listed in Table 2. After a selection based on magnitude ($M > 3.3$), and on the number of polarities available for each one, we chose to work with 18 shocks, which are singled out by a number in Table 2. The mechanisms of these 18 events were obtained by different authors and are shown in Fig. 4. They exhibit either strike-slip or compression, roughly indicating a general NW–SE compression direction. An exception is observed in the northeastern part of the region (events Nos. 1, 4, 5 and 18), where the direction of compression is rather NE–SW (Olivera et al., 1992).

A quantitative determination of the stress regime has been carried out from these focal mechanisms. The input database consists of the polarities, or senses of motion of the first P-arrivals. These measurements were obtained from seismic stations be-

Table 2
Characteristics of 30 studied earthquakes, 18 of them used for the inversion process, with the description of the epicentral parameters

Nr.	Date (day/month/year)	Time	Mag.	*Z* (km)	Latitude (ºN)	Longitude (ºE)	*N*	References
	11/03/69	18:18	4.0	5	42.7	0.7	10	Nicolas et al., 1990
	14/03/70	00:32	4.0	5?	42.52	1.70	15	Nicolas et al., 1990
	14/03/70	15:48	4.7	5?	42.52	1.68	25	Nicolas et al., 1990
	16/03/70	06:26	4.6	5?	42.54	1.71	21	Nicolas et al., 1990
	05/04/70	06:49	4.9	5?	42.47	1.66	17	Nicolas et al., 1990
	29/08/78	22:23	4.1	8	43.69	3.29	23	Nicolas et al., 1990
1	03/11/78	06:38	4.3	8	42.84	2.70	22	LDG, France (pers. commun.)
2	28/09/79	05:28	4.1	16	43.15	0.54	21	Nicolas et al., 1990
3	05/12/79	23:02	4.2	3	42.44	2.44	29	LDG, France (pers. commun.)
4	23/04/81	15:53	4.5	1	42.90	2.05	23	Gallart et al., 1982
5	23/12/82	14:48	4.1	6	43.00	3.81	31	Nicolas et al., 1990
	24/12/82	00:06	4.0	5	42.55	0.50	21	Nicolas et al., 1990
6	20/07/83	19:08	3.9	2	42.38	2.25	17	Gallart et al., 1985
7	26/09/84	04:54	4.4	5	42.32	2.17	22	SGC, 1985–1997 (1985)
8	24/08/87	18:43	4.2	7	40.95	1.57	18	SGC, 1985–1997 (1988)
9	20/02/88	16:38	3.6	1	42.36	1.46	26	LDG, France (pers. commun.)
10	16/03/88	04:33	3.8	8	42.34	2.20	41	LDG, France (pers. commun.)
11	06/01/89	19:33	4.9	11	42.99	0.17	44	LDG, France (pers. commun.)
12	05/08/90	21:32	3.7	1	42.27	1.09	18	SGC, 1985–1997 (1991)
13	15/12/91	11:50	4.2	12	40.98	2.06	30	SGC, 1985–1997 (1992)
14	19/03/92	18:53	4.2	2	42.23	2.06	39	SGC, 1985–1997 (1992)
	25/07/92	22:01	3.1	12	42.79	1.22	13	SGC, 1985–1997 (1993)
	24/08/92	22:23	2.8	1	42.27	2.32	13	SGC, 1985–1997 (1993)
	03/09/92	03:12	3.3	11	41.65	2.17	17	SGC, 1985–1997 (1993)
	02/10/92	23:06	3.2	4	42.43	1.86	13	SGC, 1985–1997 (1993)
	15/12/92	22:27	3.1	9	42.65	1.06	13	SGC, 1985–1997 (1993)
15	08/10/93	02:09	3.3	3	42.43	2.13	36	SGC, 1985–1997 (1994) (composed mechanism)
16	26/09/94	05:38	4.2	10	41.41	2.55	35	SGC, 1985–1997 (1995)
17	15/05/95	15:37	4.6	14	40.84	1.52	30	SGC, 1985–1997 (1996)
18	18/02/96	01:45	5.2	8	42.79	2.54	82	SGC, 1985–1997 (1997)

Nr. is a reference number for the selected events for the inversion process; *N* is the number of available polarities; sources of focal mechanisms are indicated in References.

longing to Instituto Geográfico Nacional (IGN), LDG, Observatoire de Midi Pyrénées of Toulouse (OMPT) and SGC, with the addition of data from other distant networks in case of strong earthquakes. Most of the readings were directly performed on copies of the original records. The LDG gives both, the polarities of P_n and P_g, but we only considered the first arrival. Thus we finally had a set of 431 polarities to invert for the stress tensor.

4.2. Stress tensor inversion from polarities

Given the heterogeneity of original determinations of focal mechanisms, we decided to start all over again by making a homogeneous processing of all earthquakes. We recalculated take-off angles by using a common standard velocity model as a function of depth. Thus, we selected a 30 km thick crust with a velocity gradient of 0.083 s^{-1}, and a gradient of 0.000185 s^{-1} for the half space. The initial velocity at the free surface is 5.0 km/s, and the velocity discontinuity at the Mohorovicic is 0.5 km/s. The inversion procedure was done by the method of Rivera and Cisternas (1990), namely looking for a common stress tensor, and for the fault planes for each event, which explain better the observed polarities. A maximum likelihood function, which weighs the observed polarities according to their distance to the nodal planes, is optimised. The inverted parameters are: the orientation of principal axes of stress (three parameters), the seismic shape factor of the stress deviator defined by $R_s = (\sigma_z - \sigma_x)/(\sigma_y - \sigma_x)$ (one parameter), and the orientation of the fault plane for each earthquake (two parameters per event). In general, we make the inversion with a large number of data values. In order to avoid instabilities, we used initial values of inversion which explore well all regions of the model space. Thus, the Euler angles, which give the orientation of the principal axes of stress, are chosen to cover all possible solid rotations. The shape factor of the deviator are given initial values of -1.0, 0.5 and 2.0, which correspond to typical regimes in compression, strike-slip and extension. The initial orientation of fault planes are changed by steps of 10° in latitude and longitude.

The output of the program, besides the stress shape and orientation, gives the pole of each fault plane with the error ellipse corresponding to one standard deviation, together with the orientation of striation on the fault planes. Unstable solutions are indicated by a star, meaning that the nodal planes are close to the principal axes of stress.

4.3. Results of the inversion

The output of the inversion leads to two kinds of models with similar characteristics. The results are good in both cases, since 86% of the polarities are correctly predicted, and the likelihood is close to 92%. The difference between both models comes out of the fact that most of the incorrect polarities are close to the nodal planes. The first solution (solution A) gives an intermediate regime (strike-slip) with a shape factor $R_s = 0.4$, and consequently σ_1 oriented almost N–S, σ_3 oriented almost E–W and σ_2 vertical. The second model (solution B) corresponds to a tri-axial compression with a shape factor $R_s = 0.1$, with the same orientation of σ_1 as before, but with σ_2 and σ_3 interchanged. The focal mechanisms obtained after inversion (Fig. 5) are quite varied, with predominant strike-slip and weaker normal or reverse components. The mechanisms are very similar for both stress models, except for three events. Events 10 and 11 show a solution in strike-slip for model A, and one in reverse faulting for model B. Event 6 shows a vertical motion for model A, and a strike-slip for model B. Besides these differences, events Nos. 2, 13, 16 and 17 interchange fault and auxiliary planes when passing from one model to the other.

The 18 focal mechanisms and the two alternative stress tensors are plotted in Fig. 6. Ten are in the Pyrenees, four in the northeastern part of the studied area and four in the southern part of the coastal area. The small number of events available on each region does not allow the separate inversion of a local stress tensor for each region. These focal mechanisms are slightly different from those previously obtained (Fig. 4), the general tendency of the common inversion being to increase the number of cases in strike-slip, as it is shown in Table 3.

5. Discussion and conclusions

The eastern part of the Pyrenean range had a different tectonic evolution since Late Eocene time,

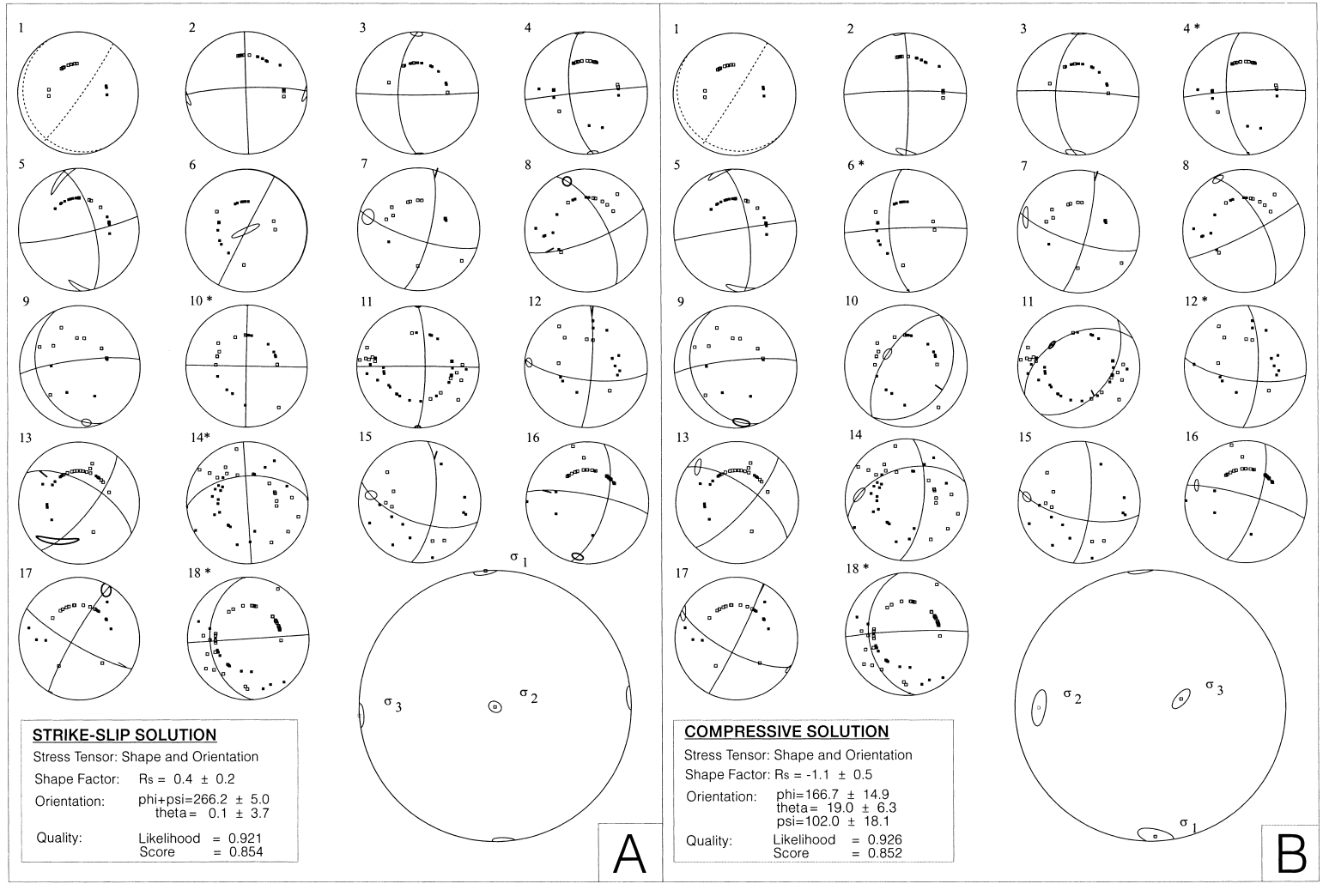

Fig. 5. Inversion results: focal mechanisms and stress tensor solutions. (A) Strike-slip regime. (B) Compressive regime. The parameters of the tensor solutions are shown together with the quality of the solutions. Fault planes and polarities are shown in the focal mechanism solutions. Fault planes are plotted in continuous lines except when the uncertainties are too large (dotted lines). Whenever it is possible to select which one of the nodal planes is the fault plane, then the direction of striation is plotted on the fault (7A, 8A, etc.). Ellipses indicate the uncertainty of the pole of one of the planes. Unstable solutions, namely those which have nodal planes which are close to principal axes of stress, are singled out by a star.

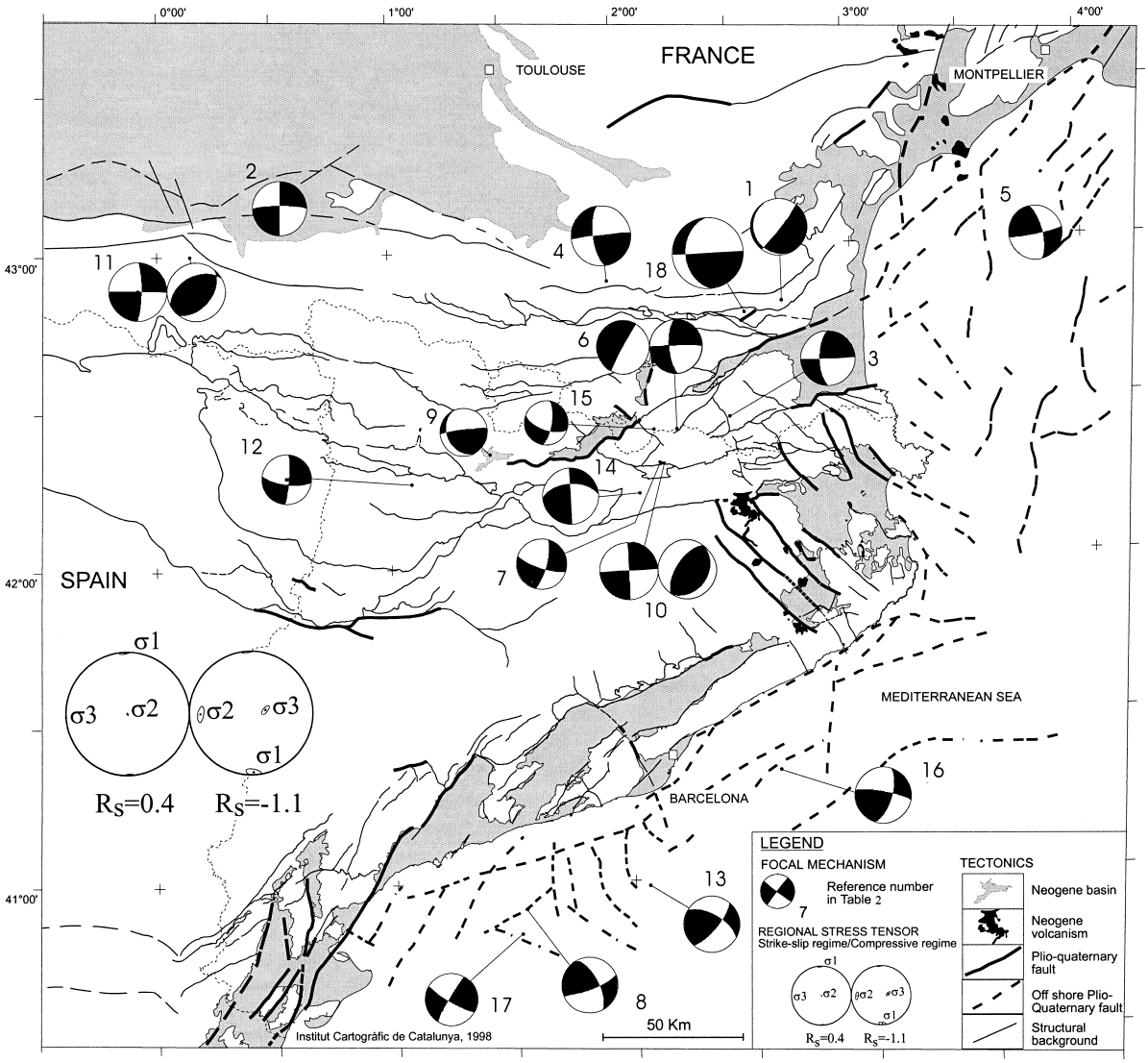

Fig. 6. Regional stress tensors and focal mechanisms obtained by the inversion process. When two focal mechanisms are plotted, the right side corresponds to the reverse stress tensor solution (Nos. 6, 10 and 11).

as compared to the central and western Pyrenees (Simón, 1984; Cortés et al., 1996), due to the influence of the European Neogene rifting episode that affected this specific area (Roca and Guimerà, 1992).

Since that time, the tectonic regime in the western part of the Mediterranean Sea gradually changed from extension to compression due to the effects of the approximately N–S convergence between the African and European plates. In fact, Western Europe is characterised by an almost homogeneous orientation of the maximum horizontal compression S_h originated from the ridge push and continental collision forces (Müller et al., 1992; Müller et al., 1997).

The orientation of the maximum horizontal compression in the northeasterm part of the Iberian Peninsula deduced from breakouts measurements shows a direction NE–SW to NNE–SSW (Jurado, 1996; Jurado and Müller, 1996).

We have produced a new data set including microtectonic analysis and instrumental seismology, in

Table 3
Distribution of the 18 events used for the inversion process, classified by the type of focal mechanisms obtained individually and after the inversion process [a]

Focal mechanism	Strike-slip	Reverse fault	Normal fault
Individual	11	6	1
After inversion	15.5	2.5	0

[a] The events with two possible solutions have been counted as a half unit.

order to analyse the regional state of stress in south-western France, eastern Pyrenees and Catalonia. This data set already includes known observations and new measurements of focal mechanisms and fault striations.

First, the inversion of the whole set of polarities of first arrivals of seismic waves from different earthquakes, corresponding to the seismic records which were available, permitted the determination of some parameters of the stress field, under the assumption of homogeneity at the regional scale. In fact, the population of earthquakes used for the determination of focal mechanisms and the stress regime corresponds to events that are of moderate size and not so numerous as to produce well constrained inversions. The presence of two alternative solutions with the same degree of confidence, suggests either the presence of more than one stress regime, or that the data set is not as complete as to single out the best one. One of the factors which may play a role in the conditioning of the problem, is the heterogeneous nature of the crustal structure in the Pyrenees, which might induce strong perturbation in the path followed by rays, hence in the take-off angles related to polarities. More precisely, one of the solutions has σ_3 oriented E–W and the other one σ_3 vertical. This ambiguity may be explained by the absence of focal mechanisms with submeridian fault planes and intermediate slopes (30º to 60º). In fact, if we had observed fault planes with those orientations, then we had been able to discriminate between these two models, since they behave in normal faulting for one of the models and in reverse faulting for the other.

On the other hand, the inversion of the collection of fault striation data led to an estimation of the main characteristics of the regional stress field in Plio-Quaternary times. The representativity of these data could be contested due to their in-homogeneous geographic distribution on the large area concerned. Indeed, most of these sites are located along the major structures which border the Neogene basins, north and south of the axial zone. Nevertheless, it has been observed in other tectonic regions that the regional stress tensor does not change in a significant way, unless there is a strong change in boundary conditions.

The observed fault planes frequently show the reactivation in reverse faulting of Neogene normal faults. We retained 23 sites with real neotectonic deformation affecting Plio-Quaternary sediments. In fact, only 15 of them have enough microtectonic measurements to obtain a stress tensor, which is not enough to produce well constrained inversions. The orientation of σ_1 is stable along the whole region, but the form factors R_t of the calculated tensors suffer from uncertainties that do not permit to conclude if the regional stress field is in compression or in strike-slip regime.

Nevertheless, both inversion approaches, carried out independently, do not present contradictions. They are characterised by the noticeable constant submeridian orientation of the maximum horizontal stress, something that was not possible to deduce from the separate individual analyses conducted until now. These results indicate that the submeridian direction of the maximum horizontal stress has been stable since the Plio-Quaternary.

Thus, the present analyses of the focal mechanisms and microtectonic data enable us to confirm the evolution of the stress regime in the eastern Pyrenees since the end of the Aquitanian period. Namely, there is a change in regional stress from an extension regime, to a regime characterised either by a strike-slip or by a compression stress tensor.

Acknowledgements

We wish to thank Commissiariat à l'Energie Atomique (Institut de Protection et Sûreté Nucleaire) and CEA (LDG) for providing seismic data concerning focal mechanisms in the south of France; the Instituto Geográfico Nacional (IGN) and Observatoire Midi-Pyrénées of Toulouse (OMPT) for data from their seismic networks. We also thank Hervé Philip, Jean Claude Bousquet, Marc Calvet and Joan

Escuer for their helpful discussions in fieldwork. We are also grateful to P. Suhadolc and J. Galindo for helpful reviews of the manuscript. Financial support has been provided by the Departament de Política Territorial i Obres Públiques de la Generalitat de Catalunya, by the French–Spanish Integrated Action (Picasso 1996–97 programme) and by GEOTER.

References

Arthaud, F., Ogier, M., Seguret, M., 1981. Géologie et géophysique du golfe du Lion et de sa bordure nord. Bull. BRGM 2, 1 (3), 175–193.

Banda, E., Correig, A., 1984. The Catalan earthquake of February 2, 1428. Eng. Geol. 20, 89–97.

Bois, C., 1993. Initiation and evolution of the Oligo-Miocene rift basins of Southwestern Europe: contribution of deep seismic reflection profiling. Tectonophysics 226, 227–252.

Cortés, A.L., Liesa, C.L., Simón, J.L., Casas, A.M., Maestro, A., Arlegui, L., 1996. El campo de esfuerzos compresivo neógeno en el NE de la Península Ibérica. Geogaceta 20 (4), 806–809.

Etchecopar, A., 1984. Etude des états de contraintes en tectonique cassante et simulations de déformations plastiques (approche mathématique). Thèse d'Etat, Montpellier, 270 pp.

Etchecopar, A., Vasseur, G., Daignieres, M., 1981. An inverse problem in microtectonics for the determination of stress tensors from fault striation analysis. J. Struct. Geol. 3 (1), 51–65.

Fleta, J., Grellet, B., Philip, H., Escuer, J., Goula, X., Bousquet, J.C., 1996. Les deformacions tectòniques en els materials plioquaternaris de la depressió de Tortellà-Besalú. In: Maroto, J., Pallí, Ll. (Eds.), Geologia de la conca lacustre de Banyoles-Besalú. Quaderns 17, Centre d'Estudis Camarcals de Baryoles, Banyoles, pp. 99–112.

Gallart, J., Olivera, C., Daignières, M., Hirn, A., 1982. Quelques données récentes sur la relation entre fractures crustales et séismes dans les Pyrénées orientales. Bull. Soc. Géol. Fr. (7), XXIV (2), 293–298.

Gallart, J., Olivera, C., Correig, A., 1985. Reconocimiento sísmico de la Cerdanya (Pirineos Orientales) — Primeros resultados. Rev. Geofís. 41, 81–90.

Grellet, B., Mio, O., Carbon, D., Colomina, I., Cushing, M., Fleta, J., Goula, X., Granier, T., Michel, C., Souriau, A., 1993. Etude des déformations actuelles en relation avec l'activité sismique des failles: réseau GPS (Global Positioning System) dans l'Est des Pyrénées. 3ème Coloque National AFPS, Saint Rémy-lès-Chevreuse, Vol. 1, St 1, pp. 1–10.

Guimerà, J., 1984. Paleogene evolution of deformation in the northeastern Iberian peninsula. Geol. Mag. 5, 413–420.

Julià, R., Santanach, P., 1980. Evolución tectónica de las fosas neógenas del litoral catalán. In: Santanach, P., Sanz de Galdeano, C., Bousquet, J.C. (Eds.), Neotectónica de las regiones mediterráneas de España (Cataluña y Cordilleras Béticas). Bol. Geol. Min. XCI (II), 321–383.

Jurado, M.J., 1996. Orientaciones de esfuerzos en la corteza superior: determinación a partir de sondeos de exploración de hidrocarburos en la Península Ibérica y en cuencas adyacentes. Geogaceta 20, 150–152.

Jurado, M.J., Müller, B., 1996. Orientación de esfuerzos en el NE de la Península Ibérica: nuevos indicadores a partir del análisis de datos de sondeos. Geogaceta 19, 27–30.

Masana, E., 1995. L'activitat neotectònica a les cadenes costaneres catalanes. Thesis, Univ. Barcelona, 444 pp.

Mauffret, A., Pascal, G., Maillard, A., Gorini, Ch., 1995. Tectonics and deep structure of Northwestern Mediterranean basin. Mar. Pet. Geol. 12 (6), 645–666.

Müller, B., Zoback, M.L., Fuchs, K., Mastin, L., Gregersen, S., Pavoni, N., Stephansson, O., Ljunggren, C., 1992. Regional patterns of the tectonic stress in Europe. J. Geophys. Res. 97 (B8), 11783–11803.

Müller, B., Wehrle, V., Zeyen, H., Fuchs, K., 1997. Short-scale variations of tectonic regimes in the western European stress province north of the Alps and Pyrenees. Tectonophysics 275, 199–219.

Nicolas, M., Santoire, J., Delpech, P., 1990. Intraplate seismicity: new seismotectonic data in Western Europe. Tectonophysics 179, 27–53.

Olivera, C., Susagna, T., Roca, A., Goula, X., 1992. Seismicity of the Valencia trough and surrounding areas. Tectonophysics 203, 99–109.

Olivera, C., Riera, A., Lambert, J., Banda, E., Alexandre, P., 1994. Els terratrèmols de l'any 1373 al Pirineu: els efectes a Espanya i França. Generalitat de Catalunya, Servei Geològic de Catalunya, Monogr. 3, 220 pp.

Olivera, C., Susagna, T., Fleta, J., Figueras, S., Goula, X., Roca, A., Martel, L., Souriau, A., Vadell, M., Grellet, B., 1996. Tectonic implications of the $M > 4$ earthquakes that occurred in Catalonia–Eastern Pyrenees area in the period 1990–1996. Proc. European Seismol. Commission XXV Assembly, Reykjavik, Sept. 9–14, pp. 29–34.

Olivera, C., Redondo, E., Riera, A., Lambert, J., Roca, A., 1999. Problems in assessing focal parameters to earthquake sequence from historical investigation: the 1427 earthquakes in Catalonia. Proc. IX Asamblea Española de Geodesia y Geofísica (in press). Almería.

Olivet, J.L., 1996. La cinématique de la plaque ibérique. BCREDP, 20, Elf Aquitaine, pp. 131–195.

Pascal, J.P., Mauffret, A., Matriat, P., 1993. The ocean–continent boundary in the Gulf of Lion from analysis of expanding spread profiles and gravity modelling. Geophys. J. Int. 113, 701–726.

Philip, H., Bousquet, J.C., Escuer, J., Fleta, J., Goula, X., Grellet, B., 1991. Presence de failles inverses d'âge quaternaire dans l'Est des Pyrénées: implications sismotectoniques. C. R. Acad. Sci. 314, Sér. II, 1239–1245.

Rigo, A., Pauchet, H., Souriau, A., Grésillaud, A., Nicolas, M., Olivera, C., Figueras, S., 1997. The February 1996 earthquake sequence in the eastern Pyrenees: first results. J. Seismol. 1, 3–14.

Rivera, L., Cisternas, A., 1990. Stress tensor and fault plane

solutions for a population of earthquakes. Bull. Seismol. Soc. Am. 80 (3), 600–614.

Roca, A., 1994. La evolución geodinámica de la Cuenca Catalano-Balear y áreas adyacentes desde el Mesozoico hasta la actualidad. Acta Geol. Hisp. 29 (1), 3–25.

Roca, A., Guimerà, J., 1992. The Neogene structure of the eastern Iberian margin: structural constraints on the crustal evolution of the Valencia trough (western Mediterranean). Tectonophysics 203, 203–218.

SGC, 1985–1997. Butlletí Sismològic. Generalitat de Catalunya. Servei Geològic de Catalunya.

SGC/OMP, 1990–1996. Seismic activity in the Pyrenees. Servei Geològic de Catalunya and Observatoire Midi-Pyrénées de Toulouse, Annual Bulletin.

Simón, J.L., 1984. Compresión y distensión alpinas en la cordillera ibérica. Instituto de Estudios Turolenses, Teruel, 269 pp.

Souriau, A., Pauchet, H., 1998. A new synthesis of Pyrenean seismicity and its tectonic implications. Tectonophysics 290, 221–244.

Villeger, M., 1984. Evolution tectonique du panneau de couverture Nord-provençal (Mont Ventoux, Lubéron, moyenne Durance). Thèse Doctorat 3ème cycle, Université Paris-Sud, Centre d'Orsay.